



저작자표시-비영리-변경금지 2.0 대한민국

이용자는 아래의 조건을 따르는 경우에 한하여 자유롭게

- 이 저작물을 복제, 배포, 전송, 전시, 공연 및 방송할 수 있습니다.

다음과 같은 조건을 따라야 합니다:



저작자표시. 귀하는 원저작자를 표시하여야 합니다.



비영리. 귀하는 이 저작물을 영리 목적으로 이용할 수 없습니다.



변경금지. 귀하는 이 저작물을 개작, 변형 또는 가공할 수 없습니다.

- 귀하는, 이 저작물의 재이용이나 배포의 경우, 이 저작물에 적용된 이용허락조건을 명확하게 나타내어야 합니다.
- 저작권자로부터 별도의 허가를 받으면 이러한 조건들은 적용되지 않습니다.

저작권법에 따른 이용자의 권리는 위의 내용에 의하여 영향을 받지 않습니다.

이것은 [이용허락규약\(Legal Code\)](#)을 이해하기 쉽게 요약한 것입니다.

[Disclaimer](#)

의학 박사 학위논문

삼차원 프린터를 이용한 새로운 생분해성
담도 스텐트의 돼지 모델에서의 타당성 및
안전성 평가: 예비연구

2023년 2월

서울대학교 대학원

의학과 영상의학 전공

김재현

삼차원 프린터를 이용한 새로운 생분해성 담도 스텐트의 돼지
모델에서의 타당성 및 안전성 평가.. 예비연구

2
0
2
3
년

김재현

의학 박사 학위논문

삼차원 프린터를 이용한 새로운 생분해성
담도 스텐트의 돼지 모델에서의 타당성 및
안전성 평가: 예비연구

2023년 2월

서울대학교 대학원

의학과 영상의학 전공

김재현

Doctoral Thesis

Feasibility and safety of a novel 3D-printed
biodegradable biliary stent in an in vivo
porcine model: a preliminary study

February 2023

The Graduate School, Seoul National University

Medicine – Radiology

Jae Hyun Kim

삼차원 프린터를 이용한 새로운 생분해성
담도 스텐트의 돼지 모델에서의 타당성 및
안전성 평가: 예비연구

지도 교수 한 준 구

이 논문을 의학박사 학위논문으로 제출함
2022년 10월

서울대학교 대학원
의학과 영상의학 전공
김 재 현

김재현의 의학박사 학위论문을 인준함
2023년 1월

위원장	서 경 석	(인)
부위원장	한 준 구	(인)
위원	정 진 욱	(인)
위원	윤 현 기	(인)
위원	이 남 준	(인)

ABSTRACT

Objectives: To assess the feasibility and safety of a novel 3D-printed biodegradable biliary stent using polycaprolactone (PCL) in an in vivo porcine model

Methods: In this animal study using domestic pigs, biodegradable radiopaque biliary stents made of polycaprolactone (PCL) and barium sulfate were produced using 3D printing and surgically inserted into the common bile duct (CBD) of pigs (stent group, n=12). Another five pigs were allocated to the control group that only underwent resection and anastomosis of the CBD without stent insertion. To check the position and status of the stents and stent-related complications, follow-up computed tomography (CT) was performed every month. The pigs were sacrificed 1 or 3 months after surgery, and their excised CBD specimens were examined at both the macroscopic and microscopic levels.

Results: Three pigs (one in the stent group and two in the control group) died within one day after surgery and were excluded from further analysis; the remaining 11 in the stent group and 3 in the control group survived the scheduled follow-up period (1 month, 5 and 1; and 3 months, 6 and 2 in stent and control groups, respectively). In all pigs, no clinical symptoms or

radiologic evidence of biliary complications was observed. In the stent group (n=11), stent migration (n=1 at 3 months; n=2 at 1 month) and stent fracture (n=3 at 2 months) were detected on CT scans. Macroscopic evaluation of the stent indicated no significant change at 1 month (n=3) or fragmentation with discoloration at 3 months (n=5). On microscopic examination of CBD specimens, the tissue inflammation score was significantly higher in the stent group than in the control group (mean±standard deviation (SD), 5.63±2.07 vs. 2.00±1.73; P=0.039) and thickness of fibrosis of the CBD wall was significantly higher than that of the control group (0.46±0.12 mm vs. 0.21±0.05mm; P=0.012).

Conclusion: Despite mild bile duct inflammation and fibrosis, 3D-printed biodegradable biliary stents showed good feasibility and safety in porcine bile ducts, suggesting their potential for use in the prevention of postoperative biliary strictures.

Keywords: biodegradable stent; polycaprolactone; 3D printing; biliary stricture

Student Number: 2016-21951

목 차

영문초록.....	i
목차.....	iii
List of Tables.....	iv
List of Figures.....	v
List of Abbreviations.....	viii
Introduction.....	1
Materials and Methods.....	4
Results.....	10
Discussion.....	23
References.....	29
국문초록.....	34

List of Tables

Table 1. Grading system for the common bile duct tissue damage.....21

Table 2. Comparison of degree of tissue damage and fibrosis between stent and control groups.....22

List of Figures

Figure 1. 3D-printed polycaprolactone biliary stents. (A) Prototype stent. (B)

Final version stent.....13

Figure 2. Flow diagram of animal allocation.....14

Figure 3. Stent placement in the common bile duct (CBD). (A) Identification and exposure of the CBD (arrows). (B, C) Transverse incision of the CBD and stent insertion.....15

Figure 4. Change of the radial force in polycaprolactone (PCL) vs. polydioxanone (PDO) stents according to the degradation period.....16

Figure 5. Representative images of 1-month (A-C), 2-month (D-F), and 3-month (G-I) follow-up CT scans to evaluate the status of biodegradable stents. The scout images (A, D, G), precontrast axial images (B, E, H), and

coronal reconstruction images (C, F, I) show a radiopaque stent in the common bile duct without complications.....17

Figure 6. Two-month follow-up CT scan images showing stent fracture. (A) Scout image and (B) 3D-volume rendered image shows complete fracture of the stent (arrows). (C, D) Axial images also shows two fragments of fractured stent (arrows) within the common bile duct without any complications such as biliary obstruction or bile leakage.....18

Figure 7. Gross morphology of polycaprolactone stents 1 month and 3 months after insertion. (A) Most stents maintain color and integration, 1 month after insertion. Specimen 3 was damaged by surgical instruments during common bile duct extraction. (B) At 3 months after stent insertion, most stents show discoloration and fragmentation. Specimens 6, 7, and 8 are prototype stents.....19

Figure 8. H&E and Masson's trichrome staining of common bile ducts (CBD) from the control and stent groups. (A, B) H&E staining shows more mucinous gland hyperplasia and lymphoplasmacytic infiltration in the CBD of stent

group than that of control group. (C, D) Masson's trichrome staining of the CBD shows more prominent fibrosis (blue-colored staining of the collagen fibers) in the stent group than in the control group.....20

List of Abbreviations

LT = liver transplantation

PDO = polydioxanone

PCL = polycaprolactone

CT = computed tomography

MRI = magnetic resonance imaging

CBD = common bile duct

INTRODUCTION

Benign biliary strictures can be caused by a wide array of non-neoplastic factors, such as postoperative complications and inflammatory conditions. Iatrogenic causes such as cholecystectomy and liver transplantation (LT) are the most common causes and account for up to 80% of all benign biliary strictures (1, 2). In addition, the incidence of biliary anastomotic stricture, which is a common source of morbidity and mortality, is known to be higher in living-donor LT (LDLT) than deceased-donor LT (19–40% vs. 15–20%) (3-5). The most important aspect of biliary stricture management is achieving permanent patency and minimizing the need for repeated interventions or surgical treatments. There are several available nonsurgical methods to manage biliary strictures, including large-bore catheterization, balloon dilatation, and stent placement via endoscopic or percutaneous approaches (6-8). Although these methods are effective in treating biliary strictures, repetitive intervention sessions for catheter exchange or stent removal have a negative effect on patient compliance and quality of life.

Recently, biodegradable stents have been proposed for the treatment of benign biliary stricture (9-11). Impressively, because biodegradable stents

degrade spontaneously, no further interventions are needed, and patients can be discharged without an external biliary drainage catheter. The biodegradable stents used in previous studies were made of polydioxanone (PDO), which is often used to produce surgical sutures. However, according to a previous study (12), PDO showed a rapid decrease in the mechanical strength with a greater than 50% decrease from the initial value within 14 days. For biliary stents, the maintenance of bile duct patency is crucial; considering that approximately two-thirds of biliary complications occur within 3 months after LT (13), PDO might not be suitable for biliary stricture management. In contrast, polycaprolactone (PCL), which is a widely used biodegradable material in medical devices, maintains its mechanical strength after 60 days (12). Chang et al. (14) demonstrated that PCL maintains its weight after 70 days of degradation in human bile juice.

In addition, rapidly evolving 3D printing technology enables the manufacture of personalized medical devices (15). Regarding biliary stricture, if it is possible to create a biliary stent after evaluation of the patient's bile duct anatomy using computed tomography (CT) or magnetic resonance imaging (MRI), biliary strictures could be managed more effectively. In a previous study (16), we established a rotating rod combined with a 3D printing system

and successfully fabricated biodegradable stents with PCL for femoral-iliac artery treatment.

In this study, we assessed the feasibility and safety of a novel 3D-printed biodegradable biliary stent using PCL in an in vivo porcine model.

MATERIALS AND METHODS

Ethical statement

This study was approved by the Institutional Animal Care and Use Committee of Seoul National University Hospital (IACUC; No. 20-0096-S1A2) and was performed in accordance with the Guide from our IACUC and the National Institute of Health Guide for the Care and Use of Laboratory Animals. All animals were maintained in a facility accredited by AAALAC International (#001169) in accordance with the Guide for the Care and Use of Laboratory Animals, 8th edition, NRC (2010). All methods are reported in accordance with ARRIVE guidelines.

Development of radiopaque biodegradable biliary stent using rotating rod-combined 3D printing system

PCL ($M_w=43,000-50,000$, PolyScience Inc., Warrington, PA, USA) was used as a biodegradable material. PCL is a bioresorbable polymer that has been used in FDA-approved medical devices, such as implants, drug delivery devices, and sutures. For radiopacity of the stent, a fine powder of barium sulfate (E-Z-HD; E-Z-EM Canada Inc., Quebec, Canada) was used. Barium powder was agitated uniformly in molten PCL on a hot plate (PCL with 25% [w/w] BaSO₄, 110 °C).

A rotating rod combined with a 3D printing system composed of a driving

unit and extrusion unit was used to manufacture biodegradable stents (16). The driving unit was operated by a G-code-based robot that consists of two heads moving translationally in the z-direction on the moving parts of x and y. The rotating rod used to print the stent was mounted on a rotating axis. The extrusion unit was composed of a heater and dispenser. The heater heated the material in the syringe to 250°C. The molten material was extruded using a dispenser capable of providing pneumatic pressure from 0 kPa to 700 kPa. The extrusion volume of the material could be modified using pneumatic pressure and nozzle size. The resolution of the 3D printing system is depending on printing temperature, extrusion pressure, and moving speed. It is possible to print the polymer from 150 µm to 1.5 mm. A rod was used as the substrate to print the tubular structure. Barium-loaded molten PCL was printed on a rotating rod to fabricate a stent with a strut of 500 µm. Our prototype PCL stent was 6 mm in diameter and 6 cm in length, and its shape was capable of loading into the delivery system used for percutaneous biliary intervention (Fig. 1A). However, the surgeon had a difficulty to insert prototype stent into the common bile duct (CBD) due to high flexibility of the stent. Therefore, we changed the design of the stent to make it easier to insert surgically. Considering the variation in CBD size depending on the pig, we made the final version PCL stent with a diameter of 4 mm or 6 mm and a length of 6 cm (Fig. 1B). The PDO (Resomer® X 206 S; CAS 29223-92-5, Sigma-Aldrich, St. Louis, MO, USA) stents for the radial force comparison test were fabricated in the same manner.

Stent radial force test

The radial force of the PDO and PCL stents during degradation in normal saline at 37°C was examined. Radial force measurements of the two stents in each group (PDO and PCL) were performed after 5, 10, and 15 weeks. A compression test machine (Instron; Norwood, MA, USA) was used. The compressive velocity was 0.5 mm/s. The stent was fixed with a jig to prevent migration during measurement. Thereafter, the tubular-shaped probe compressed the middle of the stent in a cross-sectional direction to measure radial force.

In vivo animal experiment

A total of 17 domestic male pigs (age, 3 months; weight, 26–30 kg) were divided into a stent group with 1-month follow-up (n=6), stent group with a 3-month follow-up (n=6), control group with a 1-month follow-up (n=2), and control group with a 3-month follow-up (n=3) (Fig. 2). 3 of the 6 stents used in stent group with a 3-month follow-up were prototype. All other stents were final version.

All surgical procedures were performed by two experienced hepatobiliary surgeons (Y.C. and E.S.H.). Anesthesia was induced using intramuscular injection of tiletamine-zolazepam (2 mg/kg; Zoletil 50, Virbac S.A., Carros, France) and xylazine (2 mg/kg; Rompun, Bayer HealthCare, Leverkusen, Germany). Thereafter, endotracheal intubation was performed by a

veterinarian and general anesthesia was achieved using 1.5–2% isoflurane and oxygen. After thorough shaving and skin preparation, a sterile drape was applied to the area. A midline upper laparotomy was performed and the CBD was identified and exposed. The CBD was opened transversely (Fig. 3). In the control group, the CBD incision was closed with interrupted sutures using monofilaments (polydioxanone, PDS II 5-0, Ethicone, Somerville, NJ, USA). In the stent group, a 4-mm or 6-mm biodegradable biliary stent was inserted into the CBD according to the bile duct diameter (Fig. 3). When the CBD length was less than 6 cm, the stent was cut with scissors to fit the CBD. CBD incision-site closure was performed in the same manner as in the control group. The laparotomy was closed with multifilament and monofilament sutures in the peritoneum, fascia, and subcutaneous layers (polyglactin, Vicryl 0, Ethicone, Somerville, NJ, USA), and skin (nylon, Ethilon 3-0, Ethicone, Somerville, NJ, USA).

Animals were evaluated daily. Postoperative analgesia was administered via intramuscular injection of meloxicam (Metacam, Boehringer Ingelheim, Burlington, ON, Canada) at 0.4 mL/10 kg for 3 days. All pigs also received an intramuscular injection of cefazolin (Cefozolin, Yuhan, Seoul, Korea) at 20 mg/kg, twice per day for 3 days to prevent infection. Pigs underwent 1-month and 3-month follow-up CT examinations to evaluate the status of biodegradable biliary stents and the presence of postoperative complications, such as bile duct dilatation and biloma formation.

Finally, the pigs were euthanized 1 or 3 months after surgical implantation

with intravenous injection of potassium chloride (2 mmol/kg) prior to intramuscular injection of 2 mg/kg tiletamine-zolazepam (Zoletil 50, Virbac S.A., Carros, France) and 2 mg/kg xylazine (Rompun, Bayer HealthCare, Leverkusen, Germany) for sedation. The entire CBD was sharply extirpated and immersed in 10% buffered formalin for histopathological investigation.

CT acquisition

CT examinations were performed using a commercially available, 64-channel CT scanner (Discovery CT 750 HD, GE Healthcare, Waukesha, WI, USA). Only non-contrast images were obtained to prevent unexpected adverse events in pigs following contrast injection. The CT parameters were as follows: detector configuration of 0.625 mm, tube voltage of 120 kVp, tube current of 150–200 mAs, and rotation time of 0.5 s. Axial images were reconstructed using a 2.5-mm slice thickness, and coronal multiplanar reconstruction (MPR) images were obtained using 3D imaging software.

Histopathology

CBD specimens were fixed for at least 72 hours in 10% buffered formalin, processed following standard histologic procedure, and embedded in paraffin blocks. Hematoxylin and eosin (H&E) and Masson's trichrome staining were performed on 4- μ m thick sections. On H&E staining, the severity of tissue lesions suggestive of an inflammatory response of the bile

duct, including (a) epithelial hyperplasia, (b) mucinous gland hyperplasia, (c) lymphoplasmacytic infiltration, and (d) neutrophil infiltration, was graded on a scale of 0–3 (Table 1) (17). The items (a), (b), and (c) indicate chronic inflammation, while (d) reflects acute inflammation. The sum of these four item scores was calculated as the total tissue inflammation score for each specimen. On Masson's trichrome staining, the degree of fibrosis was evaluated by measuring submucosal fibrosis thickness. The mean of three measurements in the most severely fibrotic area was used as the representative value for each specimen. All histological examinations were performed by an experienced pathologist (J.K.) blinded to the specimen group.

Statistical analysis

All results are reported as mean±standard deviation. Differences in the tissue inflammation score and fibrosis thickness were compared using the Mann–Whitney U test. Statistical significance was set at $P < 0.05$. Statistical analyses were performed using MedCalc version 12 (MedCalc Software).

RESULTS

Radial force test of 3D-printed biodegradable biliary stent

The mean radial forces of PCL stents after 5, 10, and 15 weeks in 37°C normal saline were 1.47 ± 0.04 N, 1.25 ± 0.25 N, and 1.17 ± 0.16 N, respectively (Fig. 4). The radial force of the untreated PCL stent (baseline) was 1.51 ± 0.08 N. Even after 15 weeks, the radial force of the PCL stent was more than 80% of the original radial force. In contrast, the PDO stent showed a rapid decrease in the radial force, with >90% decrease in the initial value after 5 weeks (from 1.52 ± 0.10 N to 0.08 ± 0.001 N) (Fig. 4). It was difficult to measure the radial force of the PDO stents after 5 weeks because the structure was broken before measurement.

Clinical and radiologic observation

All stents (n=12) were successfully inserted into the CBD without major difficulties in surgical procedures. Partial resection and anastomosis of the CBD were easily performed in the control group (n=5).

Among the five pigs in the control group, two died without an identifiable cause during the immediate postoperative period. Of the six pigs in the stent group with 1-month follow-up, one pig died on the first day of follow-up. Autopsy revealed a retained surgical gauze with a foreign body reaction in the abdominal cavity. In the remaining 14 pigs (six pigs in the stent group with a 3-month follow-up, five pigs in the stent group with a 1-month follow-up, two pigs in the control group with a 3-month follow-up, and one pig in the

control group with a 1-month follow-up), no specific clinical symptoms or adverse events were observed during the follow-up period.

On follow-up non-contrast CT examination, there was no radiologic evidence of bile duct obstruction or leakage in any pig (n=14). Furthermore, the stents were clearly visualized as radiopaque material, which made it easy to confirm the position and condition of the stents (Fig. 5). Among the six pigs in the stent group with 3-month follow-up, in one pig, the stent disappeared on the 3-month follow-up CT. Of the five pigs in the stent group with 1-month follow-up, two pigs showed disappearance of stents on the 1-month follow-up CT. This might be due to distal migration of the stents following bile duct peristalsis. In addition, among the 11 pigs in the stent group, three pigs in the stent group with 3-month follow-up had a stent fracture on the 2-month follow-up CT (Fig. 6).

Macroscopic evaluation of 3D-printed biodegradable biliary stent

Macroscopic findings showed no definite change in color or integration of biodegradable biliary stents in the stent group at the 1-month follow-up (Fig. 7A). However, discoloration and fragmentation of biodegradable biliary stents were noted in the stent group at the 3-month follow-up (Fig. 7B).

Histopathology

Because the tissue response could vary depending on the duration of stent placement, three pigs that lost their stents during the follow-up period were excluded from the histopathologic analysis. Therefore, histopathological

examination was performed on CBD specimens obtained from 11 pigs (control group, n=3; stent group, n=8). The stent group showed significantly higher scores for mucinous gland hyperplasia, lymphoplasmacytic infiltration, and total tissue inflammation ($P < 0.05$) (Table 2) (Fig. 8). There were no significant differences in epithelial hyperplasia or neutrophil infiltration between the stent and control groups. In addition, Masson's trichrome staining showed thicker fibrosis in the stent group than in the control group (0.46 ± 0.12 mm vs. 0.21 ± 0.05 mm, $P = 0.012$) (Table 2) (Fig. 8). Regarding the stent group, there was no difference in total tissue inflammation scores between the 1-month follow-up and 3-month follow-up groups (6.0 ± 2.65 vs. 5.4 ± 1.95 ; $P = 0.763$). In addition, there was no significant difference in fibrosis thickness between stent groups at the 1- and 3-month follow-up.

Figure 1. 3D-printed polycaprolactone biliary stents. (A) Prototype stent. (B) Final version stent.

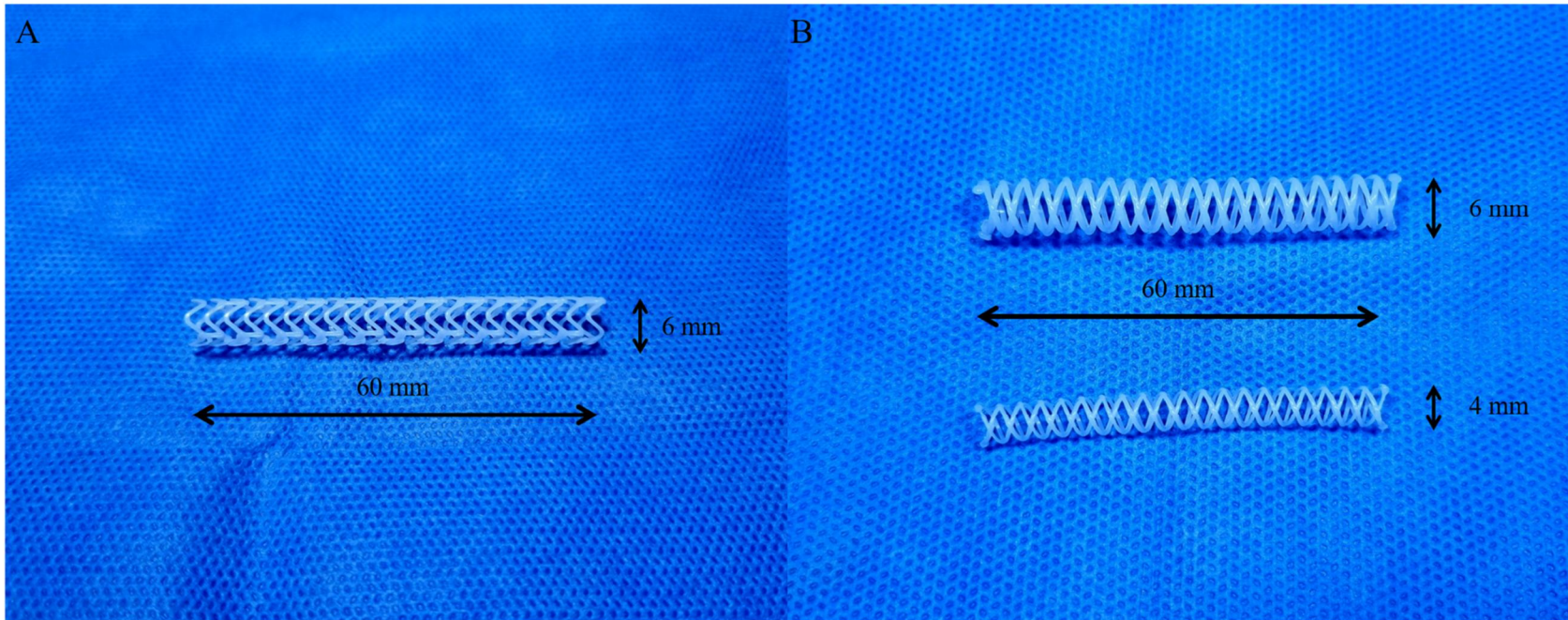


Figure 2. Flow diagram of animal allocation.

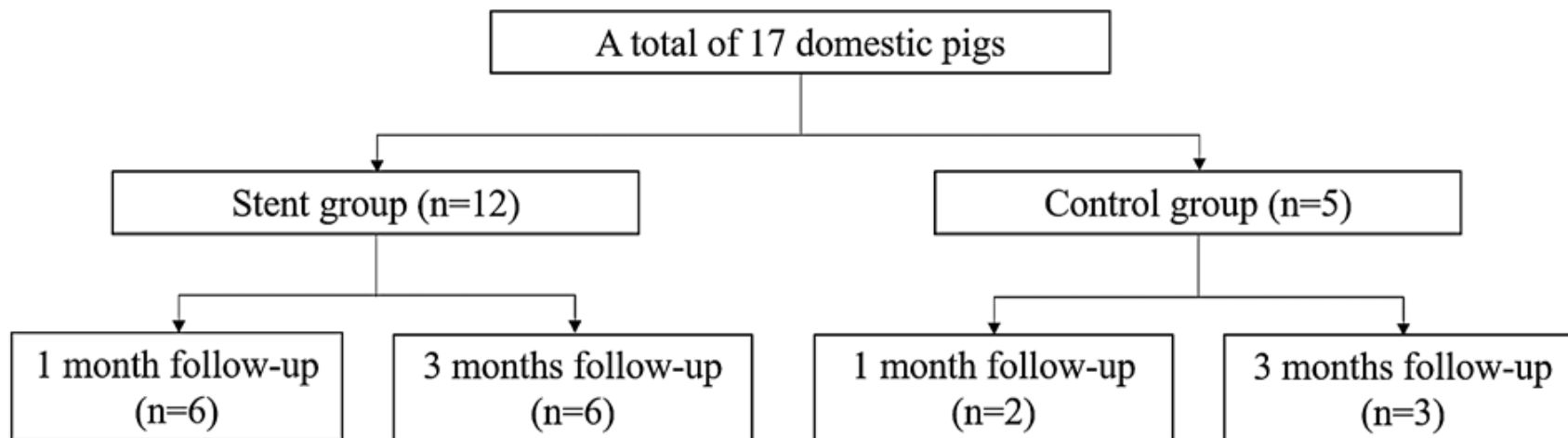


Figure 3. Stent placement in the common bile duct (CBD). (A) Identification and exposure of the CBD (arrows). (B, C) Transverse incision of the CBD and stent insertion.

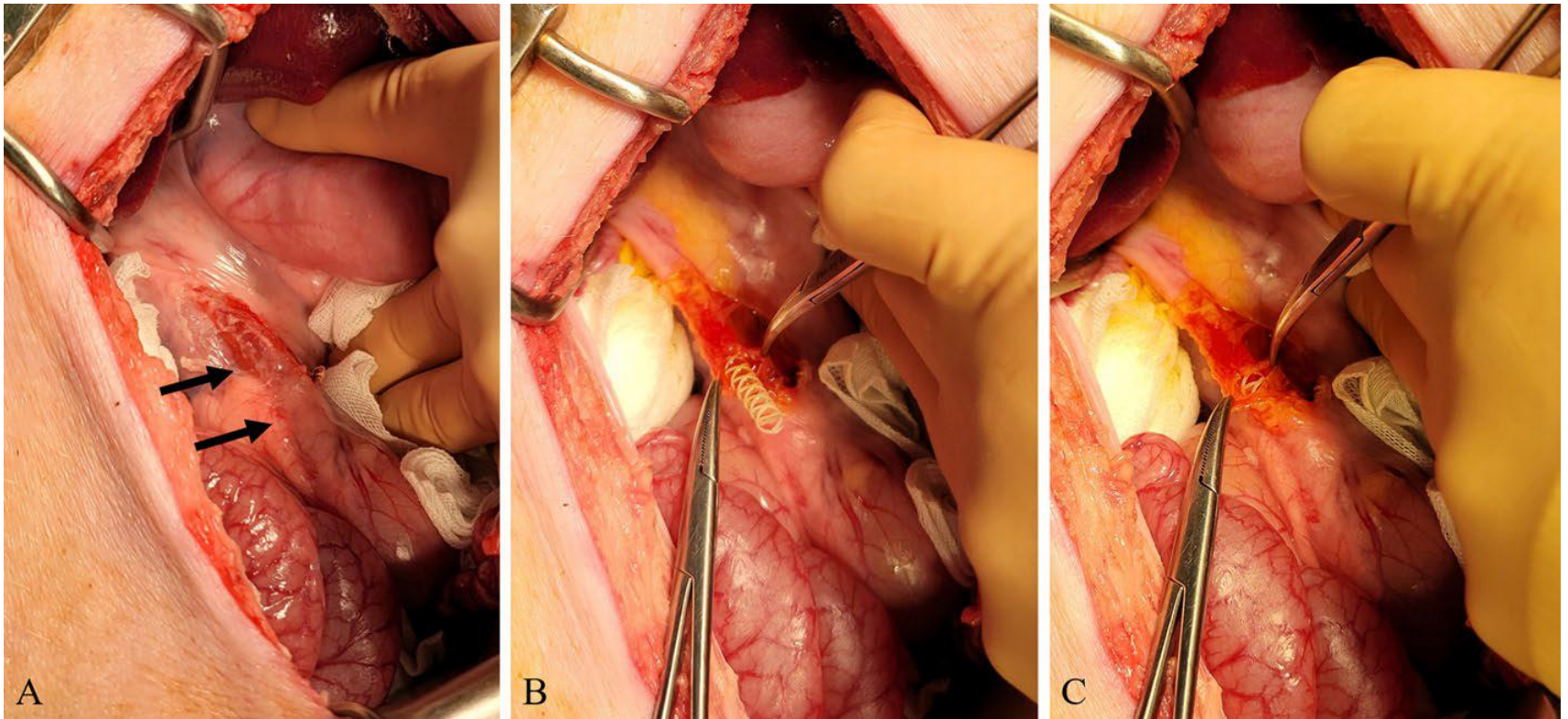


Figure 4. Change of the radial force in polycaprolactone (PCL) vs. polydioxanone (PDO) stents according to the degradation period.

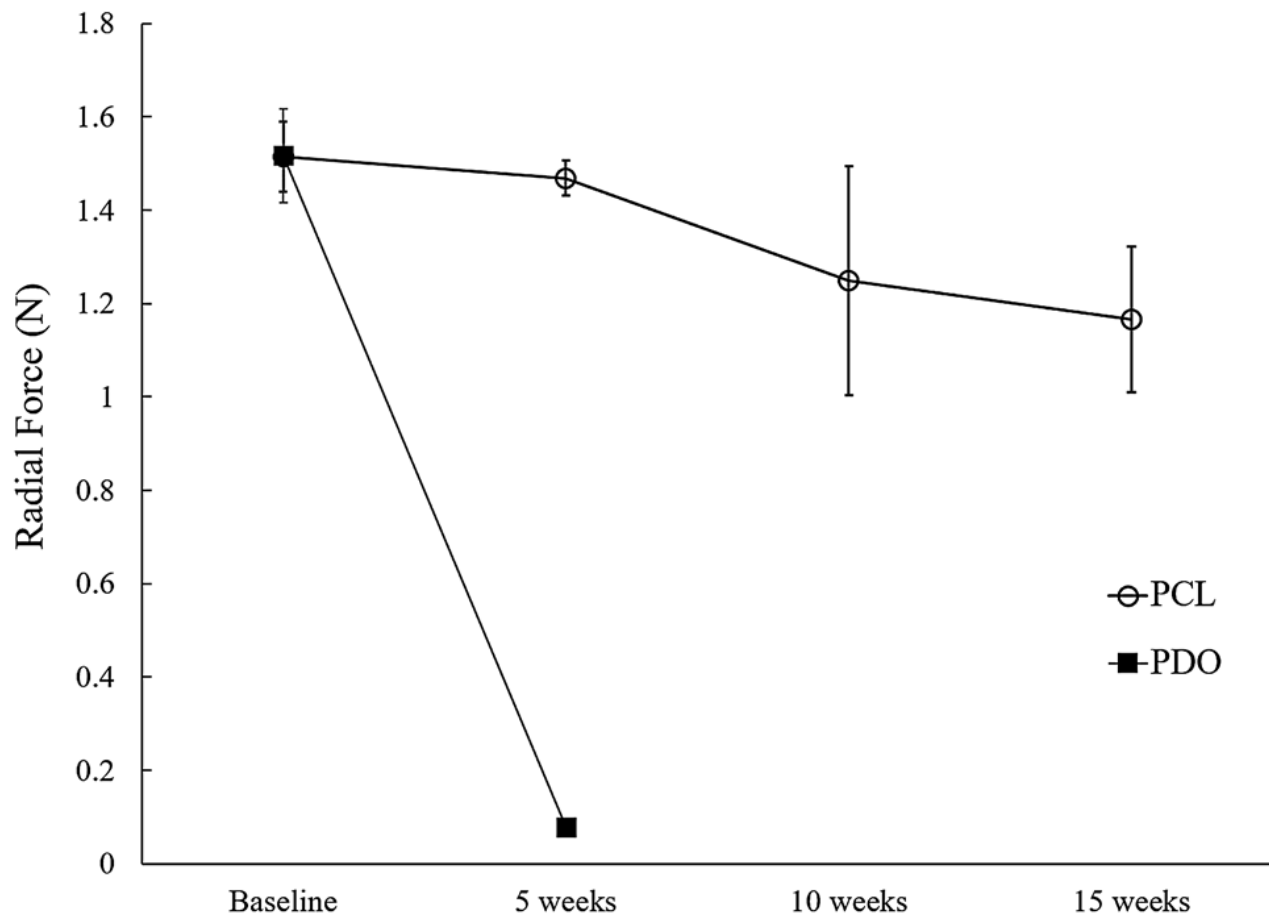


Figure 5. Representative images of 1-month (A-C), 2-month (D-F), and 3-month (G-I) follow-up CT scans to evaluate the status of biodegradable stents. The scout images (A, D, G), precontrast axial images (B, E, H), and coronal reconstruction images (C, F, I) show a radiopaque stent in the common bile duct without complications.



Figure 6. Two-month follow-up CT scan images showing stent fracture. (A) Scout image and (B) 3D-volume rendered image shows complete fracture of the stent (arrows). (C, D) Axial images also shows two fragments of fractured stent (arrows) within the common bile duct without any complications such as biliary obstruction or bile leakage.

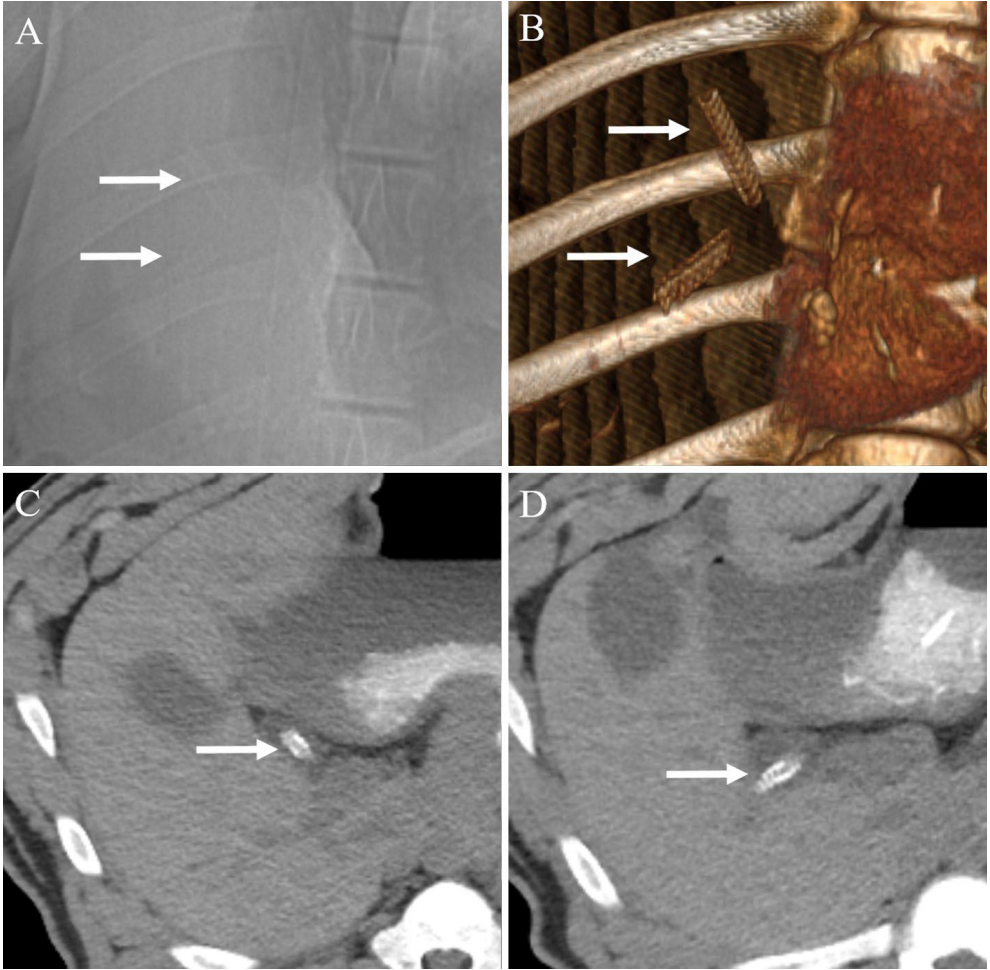


Figure 7. Gross morphology of polycaprolactone stents 1 month and 3 months after insertion. (A) Most stents maintain color and integration, 1 month after insertion. Specimen 3 was damaged by surgical instruments during common bile duct extraction. (B) At 3 months after stent insertion, most stents show discoloration and fragmentation. Specimens 6, 7, and 8 are prototype stents.

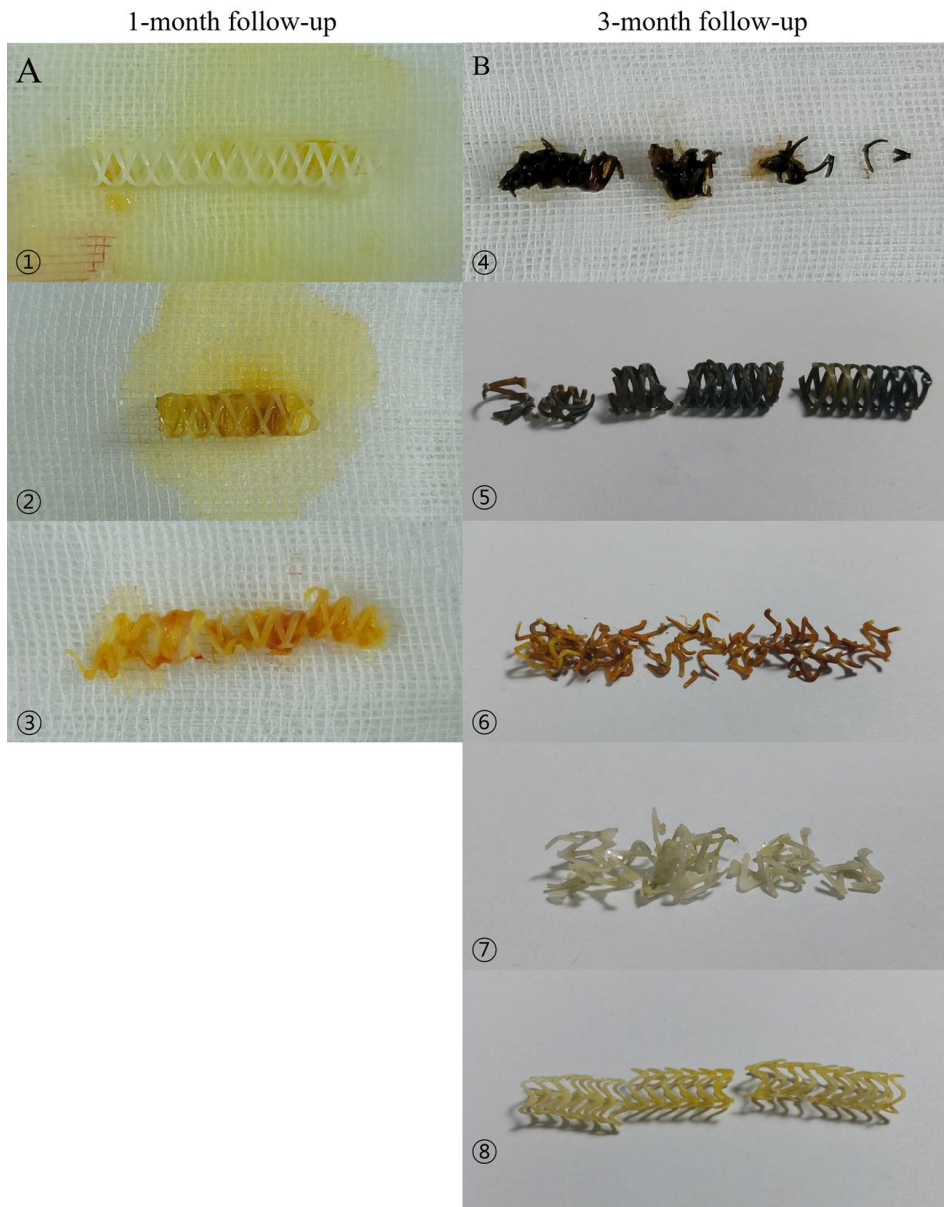


Figure 8. H&E and Masson's trichrome staining of common bile ducts (CBD) from the control and stent groups. (A, B) H&E staining shows more mucinous gland hyperplasia and lymphoplasmacytic infiltration in the CBD of stent group than that of control group. (C, D) Masson's trichrome staining of the CBD shows more prominent fibrosis (blue-colored staining of the collagen fibers) in the stent group than in the control group.

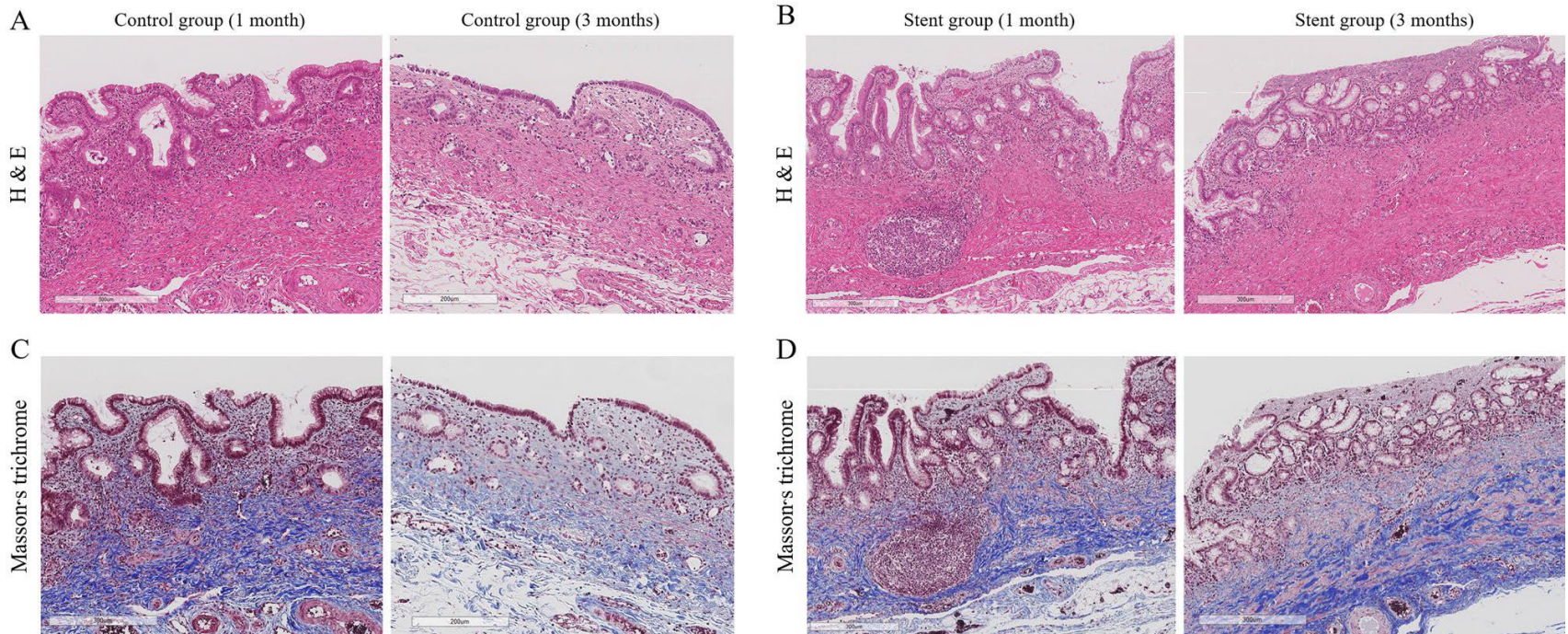


Table 1. Grading system for the common bile duct tissue damage.

Grade	Epithelial hyperplasia	Mucinous gland hyperplasia	Lymphoplasmacytic infiltration	Neutrophil infiltration
0	Mucosa lined with a single layer of columnar epithelial cells.	No significant mucinous gland hyperplasia	Spare lamina propria with occasional lymphocytes.	None
1	Mild epithelial hyperplasia.	Mild hyperplasia	Mild lymphoplasmacytic infiltration of lamina propria.	Mild
2	Moderate epithelial hyperplasia.	Moderate hyperplasia	Moderate lymphoplasmacytic infiltration of lamina propria.	Moderate
3	Severe epithelial hyperplasia	Severe hyperplasia	Severe lymphoplasmacytic infiltration	Severe

Table 2. Comparison of degree of tissue damage and fibrosis between stent and control groups.

	Stent group (n=8)	Control group (n=3)	P value
Epithelial hyperplasia	1.88±0.83	1.33±0.58	0.322
Mucinous gland hyperplasia	1.50±0.53	0.33±0.58	0.028
Lymphoplasmacytic infiltration	2.00±0.76	0.33±0.58	0.020
Neutrophil infiltration	0.25±0.46	0.00±0.00	0.361
Total tissue inflammation score	5.63±2.07	2.00±1.73	0.039
Thickness of fibrosis (mm)	0.46±0.12	0.21±0.05	0.012

Note.—Data are mean ± standard deviation.

DISCUSSION

Benign biliary strictures most commonly occur postoperatively, such as cholecystectomy and biliary anastomosis following LT. For the effective management of benign biliary strictures, repeated interventional procedures are necessary (18-20). Although it is technically demanding and burdensome, balloon dilatation and progressive plastic stent insertion showed only 80% long-term durable stricture dilatation (21). Biodegradable stents may overcome this disadvantage of conventional treatment by rendering repeated procedures for stent removal or unnecessary exchange. This study aimed to investigate the biocompatibility and safety of a novel 3D-printing biodegradable stent with PCL in a porcine model.

In our study, there were no biliary complications, such as obstruction or bile leakage, or adverse events during the 3-month follow-up period after stent placement in the CBD in a porcine model. This result suggests that our 3D printed biodegradable biliary stent made of PCL is biocompatible, at least in the porcine model, and is highly unlikely to cause problems in humans. This is similar to the results of previous studies showing good biocompatibility of biliary stents made using PDO during 8- or 20-week follow-up periods in a

porcine model (17, 22). Regarding human application, Mauri et al. (10) demonstrated the safety and effectiveness of the PDO stents for benign biliary strictures with an over 80% patency rate after monitoring 107 cases for two years.

We also demonstrated that the position and state of the biliary stent with barium could be easily evaluated on follow-up non-contrast CT. There was no difficulty in evaluating the position of the stent using only scout images. Visualization in imaging studies, such as plain radiography or CT, is one of the biggest issues in the use of biodegradable stents. Metallic stents are easily seen on plain radiography or CT because they are made of radiopaque materials. However, biodegradable materials cannot be visualized as X-rays penetrate the structure. In a previous study (22), this problem was solved by indirectly visualizing the stent by attaching gold markers to either end of the stent. However, this method has limitations when evaluating the entire stent. Because our biodegradable stent was prepared by mixing barium powder directly in the molten PCL polymer, it was easy to view the entire stent on plain radiography or CT. We used PCL with 25% [w/w] BaSO₄ to visualize the stent in plain radiography. However, no experiments were conducted on the mechanical properties of stent

according to the amount of barium. Further study is needed to clarify it.

Regarding mechanical properties, in our study, the PDO stent demonstrated a rapid decrease in radial force, with a >90% decrease from the initial value within 5 weeks. In contrast, the PCL stent maintained >80% of the initial radial force even after 15 weeks. This is similar to a previous study (12) in which PDO-dominant scaffolds lost more than 50% of their mechanical strength within 14 days, whereas PCL-dominant polymers maintained more than 90% of their initial strength after 56 days. According to several previous studies (23, 24), for the treatment of benign biliary strictures, the use of large-bore catheters maintained in place for over 6 months is necessary to achieve stricture remodeling. This finding suggests that an appropriate radial force should be applied to the stricture site for a long period to prevent stricture recurrence. Therefore, we believe that our biodegradable stents made with PCL could be more effective than PDO-based stents for the treatment of benign biliary strictures.

We found that stent migration occurred in 27.3% (3/11) of pigs, and 27.3% (3/11) of pigs exhibited stent fracture on 2-month follow-up CT. According to previous studies, stent migration occur in 16.2% of patients with fully-covered, self-expandable metal stents (CSEMS) (25) and 1.9% of patients

with PDO stents (10) for the treatment of benign biliary stricture. Because balloon dilatation after stent placement was not performed in our study, the stent might not have been fixed well, resulting in a relatively high stent migration rate. In addition, stent migration can be prevented by changing the stent design through the addition of an anchoring flap (26). Tomishima et al. (27) reported that stent fracture occurred in 7.7% (2/26) after placement of CSEMS for benign biliary stricture. Although there have been no studies on the fracture rate of biodegradable biliary stents, in a previous human study using PDO stents (28), 25% of patients developed mild cholangitis during stent indwelling. Siiki et al. reported that degradation and rupture of the stent may cause intermittent obstruction of bile flow, resulting in acute cholangitis (29). However, blockage of the large bile duct with stent fragments or stone formation may be a minor complication, as most cases can be resolved with endoscopic procedures. In addition, the use of a stent tailored to the patient's bile duct anatomy using 3D printing technology is expected to reduce the stent fracture rate. Although in our study, there were no complications related to stent fracture or fragmentation, such as bile duct obstruction or restenosis, further study is needed to develop a new PCL stent design with improved flexibility and fracture resistance.

In the gross specimens, our biodegradable biliary stents appeared fragmented at 3 months. However, considering that stents were well maintained in its original shape at 3 months follow-up CT, the process of taking the stents out of the CBD might have fragmented the fragile stents which were degraded for 3 months.

In terms of histopathology, although the stent group had significantly higher scores for mucinous gland hyperplasia and lymphoplasmacytic infiltration than those of the control group, the stent group's scores also suggested mild-to-moderate inflammation. These results are consistent with those of a previous animal study using PDO biliary stents (17), which showed mild-to-moderate inflammation during a 20-week follow-up period. In addition, fibrosis in the stent group was significantly thicker than that in the control group. According to another previous animal study using PDO biliary stents (22), the degree of fibrosis in the control group was more marked than that in the stent group at the duct-to-duct biliary anastomosis site. However, in that previous study, the fibrosis thickness of the control group was 3.84 mm, which was significantly thicker than that of our study's stent group (0.46 mm). Even the thickness of fibrosis in the stent group in our study was less than that of the control group (0.68 mm) in that study.

Therefore, although there was a difference in fibrosis thickness between the control and stent groups in our study, the degree of fibrosis in the stent group was minimal. Furthermore, according to previous studies (29, 30), mild inflammation and fibrosis in the porcine bile duct that did not cause problems such as biliary obstruction or leakage were interpreted as acceptable in terms of safety and feasibility. In order to reduce inflammation and fibrosis caused by foreign body reaction, further study is needed, such as development of drug eluting biodegradable stent.

Our study had some limitations. First, because of the expense and resources involved in conducting large animal experiments, only 17 animals were studied. It would be necessary to perform larger studies to validate our findings. Second, we only evaluated the biocompatibility of PCL stents in an animal model, and the results of a human study might be different from those of our study. Third, we did not evaluate the effectiveness of PCL stents in a benign biliary stricture model. Further studies are required to clarify whether PCL stents can improve benign biliary strictures. Fourth, although PCL requires 3 years for complete removal in the body (12, 31) and stricture remodeling requires over 6 months after stent placement (2), we only evaluated clinical and histopathologic outcomes after 3 months of

follow-up. Further studies are required to confirm the long-term effects of PCL stent placement in the bile duct. Fifth, there was no data about the radial force of the PDO and PCL stents during degradation in bile acid.

In conclusion, despite mild bile duct inflammation and fibrosis, 3D-printed biodegradable biliary stents showed good feasibility and safety in porcine bile ducts, suggesting their potential for use in the prevention of postoperative biliary strictures.

REFERENCES

1. Larghi A, Tringali A, Lecca PG, Giordano M, Costamagna G. Management of hilar biliary strictures. *The American journal of gastroenterology*. 2008;103(2):458-73.
2. Kapoor BS, Mauri G, Lorenz JM. Management of Biliary Strictures: State-of-the-Art Review. *Radiology*. 2018;289(3):590-603.
3. Akamatsu N, Sugawara Y, Hashimoto D. Biliary reconstruction, its complications and management of biliary complications after adult liver transplantation: a systematic review of the incidence, risk factors and outcome. *Transplant international : official journal of the European Society for Organ Transplantation*. 2011;24(4):379-92.
4. Williams ED, Draganov PV. Endoscopic management of biliary strictures after liver transplantation. *World journal of gastroenterology*. 2009;15(30):3725-33.
5. Martins FP, De Paulo GA, Contini MLC, Ferrari AP. Metal versus plastic stents for anastomotic biliary strictures after liver transplantation: a randomized controlled trial. *Gastrointestinal endoscopy*. 2018;87(1):131 e1-e13.
6. Janssen JJ, van Delden OM, van Lienden KP, Rauws EA, Busch OR, van Gulik TM, et al. Percutaneous balloon dilatation and long-term drainage as treatment of anastomotic and nonanastomotic benign biliary strictures. *Cardiovascular and interventional radiology*. 2014;37(6):1559-67.
7. Cantwell CP, Pena CS, Gervais DA, Hahn PF, Dawson SL, Mueller PR.

Thirty years' experience with balloon dilation of benign postoperative biliary strictures: long-term outcomes. *Radiology*. 2008;249(3):1050-7.

8. Kim JH, Gwon DI, Ko GY, Sung KB, Lee SK, Yoon HK, et al. Temporary placement of retrievable fully covered metallic stents versus percutaneous balloon dilation in the treatment of benign biliary strictures. *Journal of vascular and interventional radiology : JVIR*. 2011;22(6):893-9.

9. Mauri G, Michelozzi C, Melchiorre F, Poretti D, Tramarin M, Pedicini V, et al. Biodegradable biliary stent implantation in the treatment of benign bilioplastic-refractory biliary strictures: preliminary experience. *European radiology*. 2013;23(12):3304-10.

10. Mauri G, Michelozzi C, Melchiorre F, Poretti D, Pedicini V, Salvetti M, et al. Benign biliary strictures refractory to standard bilioplasty treated using polydioxanone biodegradable biliary stents: retrospective multicentric data analysis on 107 patients. *European radiology*. 2016;26(11):4057-63.

11. G GA, Donato P. Biodegradable versus multiple plastic stent implantation in benign biliary strictures: A systematic review and meta-analysis. *European journal of radiology*. 2020;125:108899.

12. Oh SH, Park SC, Kim HK, Koh YJ, Lee JH, Lee MC, et al. Degradation Behavior of 3D Porous Polydioxanone-b-Polycaprolactone Scaffolds Fabricated Using the Melt-Molding Particulate-Leaching Method. *Journal of biomaterials science Polymer edition*. 2011;22(1-3):225-37.

13. Pascher A, Neuhaus P. Bile duct complications after liver transplantation. *Transplant international : official journal of the European Society for Organ Transplantation*. 2005;18(6):627-42.

14. Chang H-M, Prasannan A, Tsai H-C, Jhu J-J. Ex vivo evaluation of biodegradable poly(ϵ -caprolactone) films in digestive fluids. *Applied Surface Science*. 2014;313:828-33.
15. Aimar A, Palermo A, Innocenti B. The Role of 3D Printing in Medical Applications: A State of the Art. *Journal of healthcare engineering*. 2019;2019:5340616.
16. Ha D-H, Kim JY, Park TS, Park JH, Chae S, Kim BS, et al. Development of a radiopaque, long-term drug eluting bioresorbable stent for the femoral-iliac artery. *RSC Advances*. 2019;9(59):34636-41.
17. Grolich T, Crha M, Novotny L, Kala Z, Hep A, Necas A, et al. Self-expandable biodegradable biliary stents in porcine model. *The Journal of surgical research*. 2015;193(2):606-12.
18. Lee ES, Han JK, Baek JH, Suh SW, Joo I, Yi NJ, et al. Long-Term Efficacy of Percutaneous Internal Plastic Stent Placement for Non-anastomotic Biliary Stenosis After Liver Transplantation. *Cardiovascular and interventional radiology*. 2016;39(6):909-15.
19. Kim MS, Hong SK, Woo HY, Cho JH, Lee JM, Yoon KC, et al. Optimal Intervention for Initial Treatment of Anastomotic Biliary Complications After Right Lobe Living Donor Liver Transplantation. *Transplant international : official journal of the European Society for Organ Transplantation*. 2022;35:10044.
20. You MS, Paik WH, Choi YH, Shin BS, Lee SH, Ryu JK, et al. Optimal Biliary Drainage for Patients With Biliary Anastomotic Strictures After Right Lobe Living Donor Liver Transplantation. *Liver transplantation : official*

publication of the American Association for the Study of Liver Diseases and the International Liver Transplantation Society. 2019;25(8):1209-19.

21. Costamagna G, Pandolfi M, Mutignani M, Spada C, Perri V. Long-term results of endoscopic management of postoperative bile duct strictures with increasing numbers of stents. *Gastrointestinal endoscopy*. 2001;54(2):162-8.

22. Kwon CI, Choi SH, Kim KS, Moon JP, Park S, Jeon J, et al. Preventive effect of biodegradable stents on biliary stricture and fibrosis after biliary anastomosis in a porcine model. *Annals of surgical treatment and research*. 2022;102(2):90-9.

23. Savader SJ, Cameron JL, Lillemoe KD, Lund GB, Mitchell SE, Venbrux AC. The biliary manometric perfusion test and clinical trial--long-term predictive value of success after treatment of bile duct strictures: ten-year experience. *Journal of vascular and interventional radiology : JVIR*. 1998;9(6):976-85.

24. Ludwig JM, Webber GR, Knechtle SJ, Spivey JR, Xing M, Kim HS. Percutaneous Management of Benign Biliary Strictures with Large-Bore Catheters: Comparison between Patients with and without Orthotopic Liver Transplantation. *Journal of vascular and interventional radiology : JVIR*. 2016;27(2):219-25 e1.

25. Gwon DI, Ko GY, Ko HK, Yoon HK, Sung KB. Percutaneous transhepatic treatment using retrievable covered stents in patients with benign biliary strictures: mid-term outcomes in 68 patients. *Digestive diseases and sciences*. 2013;58(11):3270-9.

26. Park DH, Lee SS, Lee TH, Ryu CH, Kim HJ, Seo DW, et al. Anchoring

flap versus flared end, fully covered self-expandable metal stents to prevent migration in patients with benign biliary strictures: a multicenter, prospective, comparative pilot study (with videos). *Gastrointestinal endoscopy*. 2011;73(1):64-70.

27. Tomishima K, Ishii S, Fujisawa T, Ikemura M, Ushio M, Takahashi S, et al. Evaluation of the Feasibility and Effectiveness of Placement of Fully Covered Self-Expandable Metallic Stents via Various Insertion Routes for Benign Biliary Strictures. *Journal of clinical medicine*. 2021;10(11).

28. Siiki A, Rinta-Kiikka I, Sand J, Laukkarinen J. A pilot study of endoscopically inserted biodegradable biliary stents in the treatment of benign biliary strictures and cystic duct leaks. *Gastrointestinal endoscopy*. 2018;87(4):1132-7.

29. Jang SI, Fang S, Nahm JH, Cho JH, Do MY, Lee SY, et al. Preclinical evaluation of endoscopic placement of a steroid-eluting metal stent in an in vivo porcine benign biliary stricture model. *Scientific reports*. 2022;12(1):8864.

30. Jang SI, Kim JH, Kim M, Yang S, Jo EA, Lee JW, et al. Porcine feasibility and safety study of a new paclitaxel-eluting biliary stent with a Pluronic-containing membrane. *Endoscopy*. 2012;44(9):825-31.

31. Beiser IH, Kanat IO. Biodegradable internal fixation. A literature review. *Journal of the American Podiatric Medical Association*. 1990;80(2):72-5.

초 록

서론: 삼차원 프린터와 폴리카프로락톤 (PCL)을 이용한 새로운 생분해성 담도 스텐트의 타당성과 안정성을 돼지 모델에서 평가하기 위한 연구이다.

방법: 본 연구에서는 삼차원 프린터를 이용하여 PLC 과 황산 바륨을 섞은 생분해성 방사선 불투과 담도 스텐트를 제작하고, 돼지의 총담관에 삽입 하였다 (스텐트 군, n =12). 또한, 다른 5 마리의 돼지는 스텐트 삽입 없이 총담관의 절제 및 문합만을 시행한 대조군에 할당하였다. 스텐트의 위치와 상태, 스텐트 관련 합병증을 확인하기 위해 매월 추적 컴퓨터 단층촬영(CT)을 시행하였다. 돼지는 수술 후 1 개월 혹은 3 개월 후에 희생되었고, 절제된 총담관 표본은 병리과 전문의가 육안적, 현미경적으로 관찰 및 분석하였다.

결과: 3 마리의 돼지(스텐트 군에서 1 마리, 대조군 2 마리)는 수술 후 하루 이내에 사망했으며 이후 분석에서 제외되었다; 나머지 스텐트 군 11 마리와 대조군 3 마리는 예정된 추적관찰 기간 (스텐트 군: 1 개월 5 마리, 3 개월 6 마리; 대조군: 1 개월 1 마리, 3 개월 2 마리) 동안

생존했다. 모든 돼지에서 담도 합병증의 임상 증상이나 영상의학적 증거는 관찰되지 않았다. 스텐트 군 (n = 11)에서는 추적관찰 CT 에서 스텐트 이동 (3 개월 째 1 마리, 1 개월 째 2 마리)과 스텐트 골절 (2 개월 째 3 마리)이 관찰되었다. 스텐트의 육안 평가 결과 1 개월 째 (n = 3)에는 유의한 변화가 없었고, 3 개월 째 (n = 5)에 변색과 단편화가 관찰되었다. 총담관 표본의 현미경 검사에서 조직 염증 점수는 대조군보다 스텐트 군에서 유의하게 높았고 (mean±standard deviation, 5.63±2.07 vs. 2.00±1.73; P=0.039), 총담관 벽의 섬유화 두께도 대조군보다 스텐트 군에서 유의하게 두꺼웠다 (0.46±0.12 mm vs. 0.21±0.05mm; P=0.012).

결론: 경미한 담관 염증 및 섬유화에도 불구하고 삼차원 프린터로 만든 생분해성 담도 스텐트는 돼지 담관에서 좋은 타당성과 안정성을 보여, 추후 수술 후 담도 협착 예방에 사용할 수 있는 가능성을 보였다고 할 수 있겠다.

주요어: 생분해성 스텐트; 폴리카프로락톤; 삼차원 프린팅; 담도 협착

학번: 2016-21951